

H. Hyodo and T. Itaya

Research Institute of Natural Sciences,
Okayama University of Science

INTRODUCTION: Grenville dike (c.a. 570 Ma) in the Mattawa area, Ontario, Canada developed a contact aureole in the tonalitic country rock. The heat released during dike intrusion seems to have created a complexed thermal history in the country rock as a secondary component was observed in the paleomagnetic results [1]. Minerals have ranges of closure temperature corresponding to their argon diffusion characteristics. Many laboratory diffusion experiments were carried out. In order to determine the characteristics under a field condition. We investigated the secondary effect of the heat on the K-Ar age system in the hornblende, biotite and feldspars samples using laser stepheating $^{40}\text{Ar}/^{39}\text{Ar}$ age experiment.

EXPERIMENTS: Rock samples were crushed, and sieved in #25-50 mesh. After ultrasonic cleaning in distilled water, single mineral grains were handpicked. The minerals were irradiated in the KUR for 24 hours at 1 MW for $^{40}\text{Ar}/^{39}\text{Ar}$ age determination. The total neutron flux was monitored by 3gr hornblende age standard [2], [3], which was irradiated in the same sample holder. In the same batch, CaSi_2 and KAlSi_3O_8 salts were used for interfering isotope correction. A typical J-value was 1.970 ± 0.017 . In stepwise heating experiment, temperature of the mineral grains was measured using infrared thermometer whose spatial resolution is 0.3 mm in diameter [4].

RESULTS: No agreement in ages or spectrum shapes are found between different sets of minerals. However, basic spectrum shapes are consistent in hornblende, biotite and K-rich feldspar minerals, respectively. These results suggest that the spectrum shapes possibly represent interaction between the thermal history and diffusion characteristics of each mineral. The process of the interactions are complicated and possibly affected by presence of fluid. An example of age spectra results were shown in Fig. 1. The higher temperature fractions (0.8 – 1.0) tend to approach the intrusion age of the dike 570 Ma. On the other hand, the lower temperature fractions have apparent excess ages with gradual decrease with increasing temperature. This spectrum shape may be caused by several processes; 1. variable excess argon pressure with time, 2. product of mineral reactions and diffusion characteristics, or combination of the two processes.

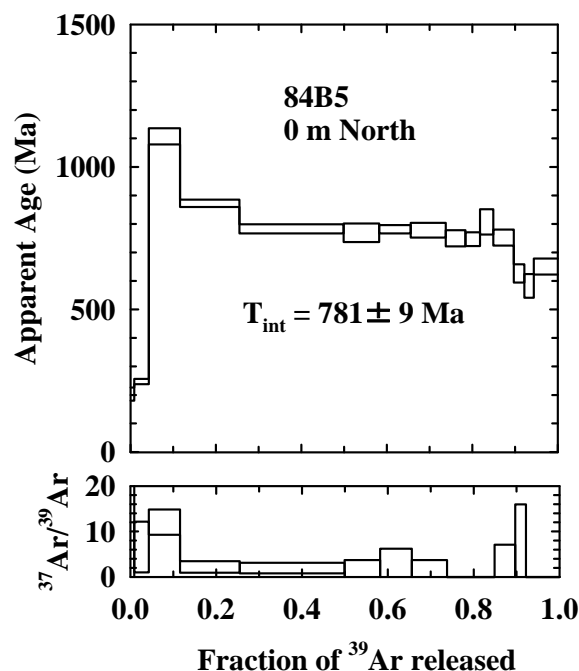


Fig. 1. $^{40}\text{Ar}/^{39}\text{Ar}$ age and $^{37}\text{Ar}/^{39}\text{Ar}$ ratio spectra of a biotite from tonalitic country rock on the contact with a Grenville dike in Mattawa, Ontario, Canada. The ratio spectra suggest a presence of relatively homogeneous mineral phase, but the age spectra have varieties of ages due to the secondary and possibly tertiary thermal events.

REFERENCES:

- [1] H. Hyodo and D.J. Dunlop, *J. Geophys. Res.* **98** (1993) 7997-8017.
- [2] G. Turner, J.C. Huneke, F.A. Podosek and G.L. Wasserburg, *Earth Planet. Sci. Lett.* **12** (1971) 19-35.
- [3] J.C. Roddick, *Geochim. Cosmochim. Acta* **47** (1983) 887-898.
- [4] H. Hyodo, S.-W. Kim, T. Itaya and T. Matsuda, *J. Min. Petr. Econ. Geol. J.* **94** (1999) 329-337.

N. Hasebe, K. Ito¹, A. Inagaki¹, H. Yamada¹ and S. Oishi

Institute of Nature and Environmental Technology, Kanazawa University

¹*Graduate School of Natural Science and Technology, Kanazawa University*

INTRODUCTION: Luminescence dating observes the natural accumulated radiation damage caused by radioisotopes such as U and Th as the form of glow after stimulation by heating or lightening. The luminescence is observed at various wavelength and emission color of luminescence can be recorded easily by using thermoluminescence color image (TLCI) analysis for samples artificially irradiated with gamma-rays [1]. When TLCI is applied to polymineral from lake sediments, the luminous mineral compositions of samples may reflect the regional characteristic and climate of the studied area. The aim of this study is to reconstruct paleoclimate change using TLCI method.

EXPERIMENTS: The boring core from Lake Hovsgol is used for the experiment. Lake Hovsgol is the largest fresh water lake in Mongolia and is located in Baikal Rift Zone at an elevation of 1645m on the southern fringes of the East Siberian permafrost zone and connected to Lake Baikal through Egiin River, a tributary of the Selenga River. Because of its location in the middle of Asian continent and high altitude, the area is likely to be more sensitive to climate change, less affected by human activities. The sediments recovered from the lake have preserved important proxy records of past environmental changes. The drilling operation was conducted in March 2004 at 50° 57' 19" N 100° 21' 32" E in a water depth of 239.3 m by Hovsgol Drilling Project Members and HDP-04 core was obtained. 136 samples were taken from the HDP-04 core for every 36 cm starting from 2.46m to the depth of 56.47m.

Each sample was treated with H₂O₂ to remove organic matter that emits no luminescence. Samples were then irradiated by gamma-ray from Co-60 with dose rate of about 1.467kGy/h at Kyoto University Research Reactor Institute. The total gamma dose were 36 kGy given for 24.5 hours on the irradiation stage, which stand off 20cm from the radiation source.

Afterwards the photograph of TLCI was taken under a constant temperature of about 230°C. Colored pixels were picked up by the software programmed in this study and then converted to numerical values. Based on [2], color index were calculated from these numerical values and then were divided into five color ranges; blue (B, 450<=B<=495nm), green (G, 495<G<=565nm), yellow (Y, 565<Y<=580nm), red (R, 580<R<=700nm) and others (Gap).

RESULTS: The average number of picked up pixels of each sample is shown in Fig. 1. The emission intensities of TLCIs were different from sample to sample, though TLCIs showed poor reproducibility based on the large standard deviations of emission intensities on the same samples. The color pixel points on CIE chromaticity diagram fell in the same region with those for calcium carbonate from Darkhad basin. The intensity showed similar fluctuation pattern to the amount of HCl-soluble-material. These observations suggest that calcium carbonate is a main luminescence emitter. When luminescence signal is observed according to grain sizes, for fine grained samples, a small number of color pixel points were found on blue-purple region apart from main cluster of pixels in the CIE diagrams (Fig.2), however, we couldn't find the concrete evidence of presence of eolian dust fractions due to few samples analyzed. The emission intensity seemed to have no relation with glaciation or insolation cycles except for several events, in which the emission intensity and the rate of red emission were decreased. However, by spectrum analysis, the emission intensity shows cycles in connection with insolation as was found in HCl-soluble-material and grain size fluctuation.

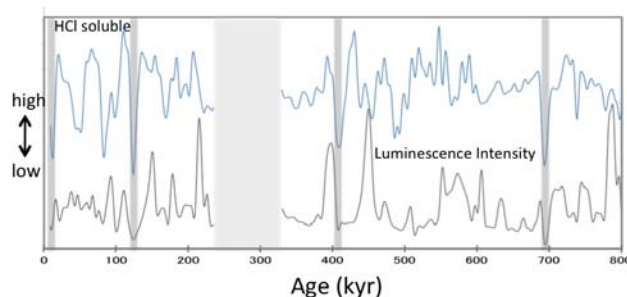


Fig. 1. The amount of HCl soluble and average luminescence intensity plotted against estimated age of the core.

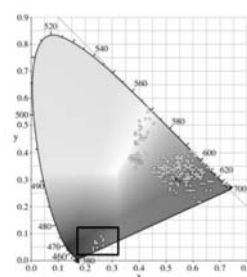


Fig. 2. An example of CIE diagram to represent luminescence color characteristics. A square indicates unusual color pixels only found in fine grained component.

REFERENCES:

- [1] T. Hashimoto et al., Nucl.Tracks16, 1, (1989)3-10.
- [2] Y. Ganzawa and K. Kubokita, Quat. Res. 40, 5, (2001) 403-413.

N. Ito, A. Mizohata and Y. Nakano¹

Frontier Science Innovation Center, Osaka Prefecture University

¹Research Reactor Institute, Kyoto University

During March to April for almost every year we observe high concentration events of atmospheric soil particles, called Kosa . Kosa is come from Chinese dessert (Gobi dessert or Takla Makan dessert). We have observed Kosa event as high concentrations higher than 100 $\mu\text{g}/\text{m}^3$ in which maximum concentration we have observed was 600 $\mu\text{g}/\text{m}^3$. We observed Kasa event at Apr. 1st and 2nd in 2007 of which concentrations were 120 and 590 $\mu\text{g}/\text{m}^3$ respectively(Fig.1). The aerosol on these days were collected and the other samples before and after these Kosa event were also collected. We have analyzed the elemental concentrations on these samples by neutron activation analysis. On this paper we will show the elemental concentration change for before and after Kosa event.

The atmospheric aerosol samples have been collected on the membrane filter every day at Osaka Prefecture University, Sakai City. The some of the samples were analyzed by neutron activation analysis. The neutron irradiations were done at Kyoto University Nuclear Reactor(KUR) on the condition showed on Table.1

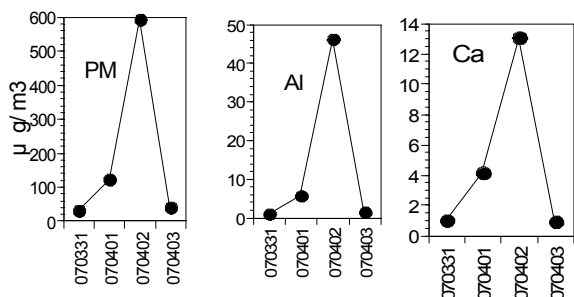


Fig.1. Concentration Change of PM,Al,Ca.

We show the concentration ratios of the mean for before and after Kosa to Kosa event on Fig.2. For the big Kosa event day, Apr. 2nd ,PM(Particle Mass concentration) increased 17times higher than before and after non-Kosa day. The elements for which concentration ratios are higher than 17 are Al,K, Ti,Sc, Mn,Fe,Co, Rb, Cs, Ba, La, Ce,Sm,Eu,Th. In those element Al, Sc,Sm,Eu,Th have high concentration changes.

Table 1. Neutron activity analysis condition at KUR.

Elements for analysis	Irradiation	
	Station	Period
Al, Cl, Ca, Ti, V, Mn	Pn-1	2min in 1MW
K,Sc,Cr,Fe, Co, As, Rb, Sb, Cs, Ba, La, Ce, Sm,Eu, W, Th	Pn-2	2h in 1MW

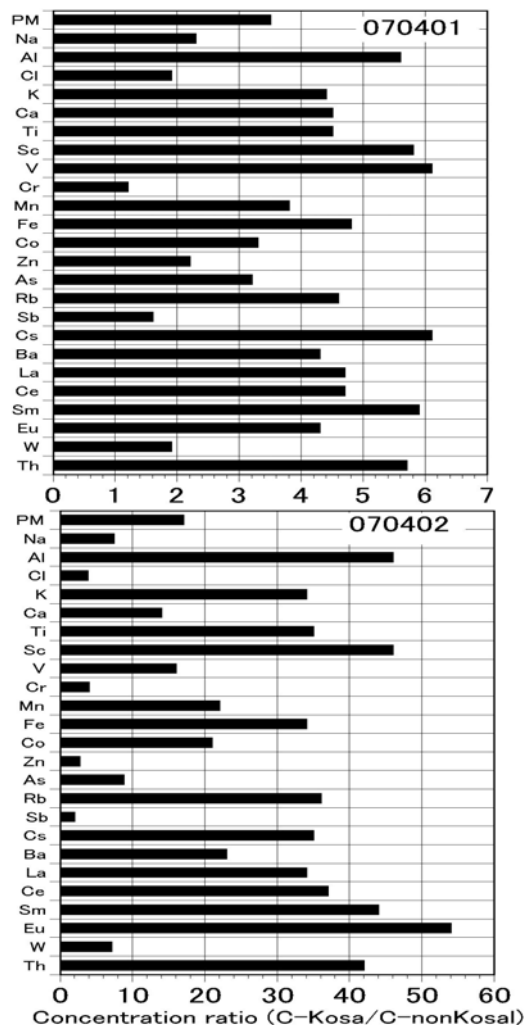


Fig.2. Ratios of concentration between Kosa day (070401 and 070402) and non Kosa day,average by before and after Kosa day.

CO5-4 Study on Thermal History of Hydrothermally Altered Rocks Based on Fission Track Dating

H. Ohira and A. Takasu

Department of Geoscience, Shimane University

INTRODUCTION: Fission track (FT) dating was applied for several Cretaceous granitic rocks (the Itoshima Granodiorite and Sawara Granite) in the Gokayama area, northern Kyushu, to estimate thermal history of hydrothermal activity. Abandoned workings at several gold prospects occur within the Sawara Granite and the rocks around the gold prospects have been altered by hydrothermal activity. This hydrothermal alteration is characterized by the appearance of chlorite, illite and pyrite. The maximum temperature of the alteration has been estimated to be more than 200°C, based on fluid inclusion analysis [1]. Since FT in minerals have relatively lower closure temperature (track retention temperature), 240°C for zircon and 100°C for apatite, apparent fission track ages may indicate a timing of hydrothermal activity or a period which sample cooled below above closure temperatures during cooling process.

EXPERIMENTS: Rock samples were collected from the above granitic rocks. Zircon and apatite were separated by conventional magnetic and heavy liquid separation techniques. Zircons were mounted in PFA Teflon and apatites in epoxy resin (Specific-20), and then polished to reveal a complete internal surface. Zircons were etched in an NaOH-KOH eutectic melt at 225°C for 25-35 hours, whereas apatites were etched in a solution of 7% HNO₃ at 25°C for 30-35 seconds[2]. Samples were irradiated at pneumatic tube of graphite facility (Tc-pn) of Kyoto University Reactor (KUR). After irradiation, external detectors (mica) were etched in 46% HF at 25°C for 9-10 minutes (for mineral mounts) and for 20-50min (for NIST-612). FT densities were measured at 1000× magnification with a dry objective. The zeta values used were 367.1±4.1 for zircon and 313.5±5.1 for apatite.

RESULTS: A schematic cooling history based on zircon and apatite FT ages and their closure temperature is shown in Fig. 1. Zircon and apatite FT ages range from 83.1-62.0Ma and 18.2-3.8Ma, respectively. The FT ages and previously reported Rb-Sr data [3] define typical cooling history for the granitic basement. Only the apatite FT age of the Itoshima Granodiorite determined here show relatively older age 18.2 Ma. This age records the time that the sample cooled below 100°C, and is concordant with the range of apatite FT ages from granitic rocks in the western block of the

Fukuoka area [4]. The cooling curve passes through 300°C at 88-89 Ma, 220°C at 83-62 Ma and 100°C at 18 Ma. This is probably a typical cooling history of basement granitic rocks in the study area.

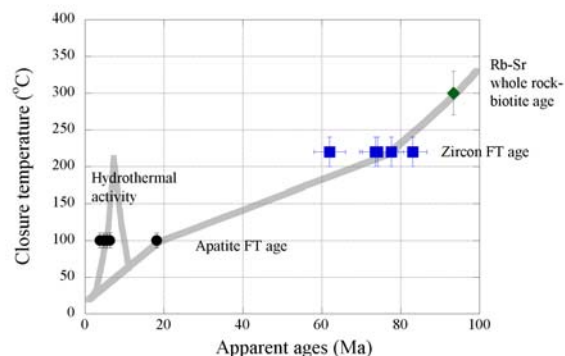


Fig. 1. Schematic cooling history of rocks illustrated based on measured mineral ages against established closure temperatures.

However, the whitened altered rock from the Ono gold prospect gives an apatite FT age of 6.3 Ma and other altered rocks show a range from 5.4 to 3.8Ma. Almost apatites show significantly younger ages comparing with that of the Itoshima Granodiorite (18.2 Ma). These younger apatite ages (6.3-3.8Ma) probably indicate the period of hydrothermal activity and suggest that the activity continued through to 3.8 Ma in some places. The hydrothermal alteration was probably caused by infiltration of hot water passing through the fracture zone that lies parallel to the local fault system [5].

REFERENCES:

- [1] M. Yuhara *et al.*, Fukuoka Univ. Science Reports, **35** (2005), 49-73 (in Japanese with English abst.).
- [2] C.W. Naeser, USGS Open-file report 76-190 Part II Laboratory procedure, (1976) 1-28.
- [3] M. Owada *et al.*, The Memoirs of the Geological Society of Japan, **53** (1999), 349-363.
- [4] T. Ishii *et al.*, Fission Track News Letter, **13** (2000), 53-56 (in Japanese).
- [5] M. Yuhara *et al.*, Fukuoka Univ. Science Reports, **36** (2006), 55-67 (in Japanese with English abstract).

CO5-5 Soil Remediation by Photolysis Reaction and Elution with Organic Substances

T. Kubota, T. Ohta and Y. Mahara

Research Reactor Institute, Kyoto University

INTRODUCTION: The strategy of soil remediation is to detoxify and to remove toxic substances. Harmful organic substances, such as PCB and dioxin, can be detoxified through irradiation of electron and photon of less than 8 MeV without inducing radioactivity. These low-energy electrons have been generated with a new operation to KURRI-LINAC generating high-energy electron of 30 MeV in the normal operation [1]. The evaluation of irradiation field would be required for degradation of harmful organic substances. In the case that pollutant is heavy metal the pollutant is required to be removed by some methods. Heavy metals would be effectively removed by chemical reagents. Decontamination reagents which are high environmental load and expensive should be avoided, however their removal efficiency is high. Natural decontamination reagents can be easily extracted from inexpensive plant wastes. We have investigated the remediation strength of fulvic and humic substances extracted from fallen cherry leaves to sand samples loaded with gadolinium, which is analog to trivalent actinides, such as plutonium and americium, in aqueous solution. In this paper we report the evaluation of irradiation field at KURRI-LINAC and the comparison of remediation strength between natural and artificial reagents.

EXPERIMENTS: Beam spot position is changed by low-energy beam regulation. This position was easily determined with a poly vinyl chloride sheet irradiated by electron and photon beam. An irradiation spot on the sheet first turned to green and then developed to brown. Irradiated sheets left for 20 min after irradiation were scanned to evaluate irradiation strength.

Natural organic substances extracted from fallen cherry leaves with NaOH treatment were separated to fulvic and humic substances with HCl treatment. Sand samples loaded with gadolinium-153 were washed with fulvic and humic solutions. The remediation strength of both substances was investigated with a comparison of EDTA and HCl. This strength was evaluated with a distribution of gadolinium-153 between sand and solution.

RESULTS: Though the beam spot in general was concentrically distributed, the spot on PVC sheet purposely disturbed was scanned to draw a contour map of irradiation (Fig. 1). This contour map was easily obtained and provided information on beam regulation and irradiation field.

The elution property of gadolinium from sand samples is shown in Fig. 2. Without organic substances gadolinium was significantly eluted only below pH 3. With organic substances gadolinium was effectively eluted around weak acidic region. A similar elution property is shown at 15 ppmC of EDTA, 2000 ppmC of humic acid, and 4000

ppmC of fulvic acid [2-3]. These solution conditions provided that 60 % of gadolinium was eluted at one treatment and this result was comparable to 0.01 M HCl.

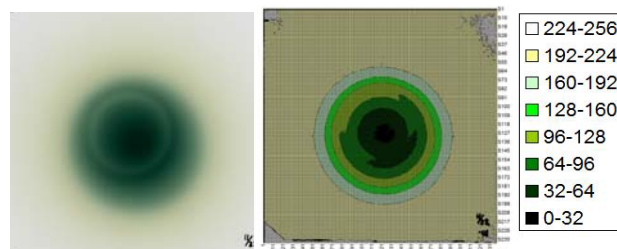


Fig.1. Irradiated PVC sheet (left) and contour map of irradiation (right).

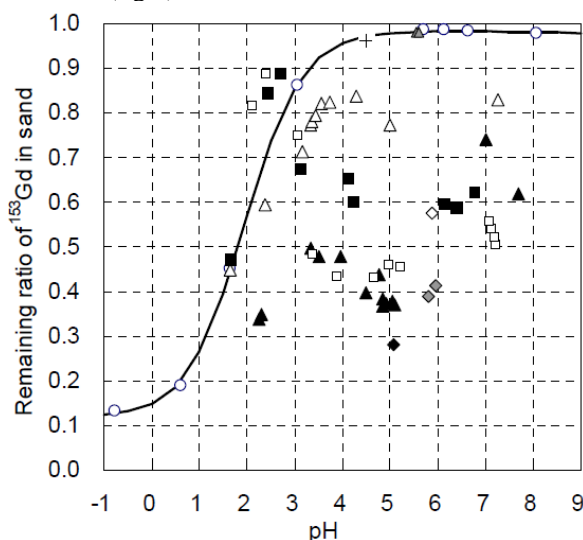


Fig.2. Remaining ratio of ^{153}Gd in sand after elution with inorganic and organic solutions. \circ : Inorganic solution. \triangle , $+$, Δ , and \blacktriangle : Fulvic acid of 11, 110, 670, and 4000 mgC/L, respectively. \blacksquare and \square : Humic acid of 670 and 2000 mgC/L, respectively. \diamond , \blacklozenge , and \blacklozenge : EDTA solution of 1.5, 15, and 150 mgC/L, respectively.

REFERENCES:

- [1] T. Kubota *et al.*, Proceedings of the 25th International Linear Accelerator Conference (LINAC2010), 67-69, (2011).
- [2] T. Kubota, Proceedings of the third Asian and Oceanic Congress on Radiation Protection (AOCRP-3), (2010).
- [3] T. Kubota, Proceedings of the 13th International Conference on Environmental Remediation and Radioactive Waste (ICEM2010), ICEM2010-40122, (2010).

CO5-6 Study of Earth and Planetary Matters by Thermoluminescence

K. Ninagawa

Department of Applied Physics, Okayama University of Science

TL OF ORDINARY CHONDRITES: Induced TL (thermoluminescence), the response of a luminescent phosphor to a laboratory dose of radiation, reflects the mineralogy and structure of the phosphor, and provides valuable information on the metamorphic and thermal history of meteorites. Especially the sensitivity of the induced TL is used to determine petrologic subtype of unequilibrated ordinary chondrites [1]. Natural TL, the luminescence of a sample that has received no irradiation in the laboratory, reflects the thermal history of the meteorite in space and on Earth. Natural TL data thus provide insights into such topics as the orbits of meteoroids, the effects of shock heating, and the terrestrial history of meteorites [2]. Natural TL properties are usually applied to find paired fragments [3-5]. Recently we have measured induced and natural TL properties of Yamato unequilibrated ordinary chondrites, which sampling positions were measured by GPS. In this year we measured TL of additional fourteen (H3: 7, L3: 7) chondrites from Y981121 to Y981301 of Japanese Antarctic meteorite collection. Then we have measured totally TL of fifty-six Yamato unequilibrated ordinary chondrites with GPS sampling positions.

PRIMITIVE ORDINARY CHONDRITES: Most of the chondrites had TL sensitivities over 0.1 (Dhajala=1), corresponding to petrologic subtype 3.5-3.9. This time one chondrite, Y981221 (H3) was revealed to be a primitive ordinary chondrite, petrologic subtype 3.2-3.4. Then we recently found primitive chondrites, Y983183(LL3.0), Y983278(LL3.3-3.4), Y981221(H3.2-3.4) under 3.4 as shown in Fig.1. They are particularly significant in

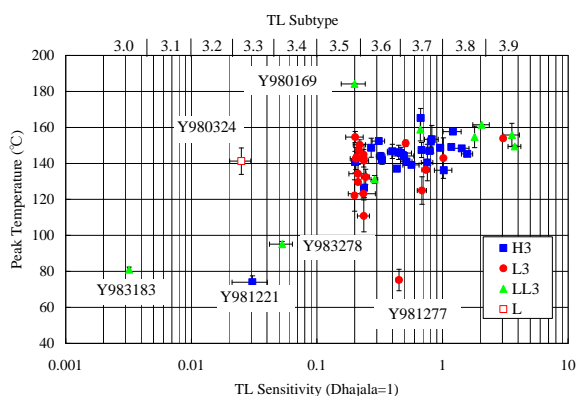


Fig.1. Induced Peak Temperature vs. TL Sensitivity to search primitive ordinary chondrites. Y980324 is a shocked chondrite.

understanding the nature of primitive material in the solar system.

PAIRING: Natural and induced TL properties were also applied to find paired fragments, and we found forty-one potential paired fragments by TL, satisfying the criteria of 1) the natural TL peak height ratios, LT/HT, should be within 20%; 2) that ratios of raw natural TL signal to induced TL signal should be within 50%; 3) the TL peak temperatures should be within 20°C and peak widths within 10°C. Some of the forty-one paired fragments comprised large three groups. Considering distances between the paired fragments, five fragments were eliminated from paired fragments.

TL SPECTRA OF A CR CHONDRITE: A Chondrite, Y981208, showed different induced TL glow curves from the ordinary chondrites with 150 and 250 °C peaks. It also had the same 400 nm peaks, different TL spectra from ordinary chondrites as shown in Fig. 2. This reflect different origin and metamorphic history from the ordinary chondrite.

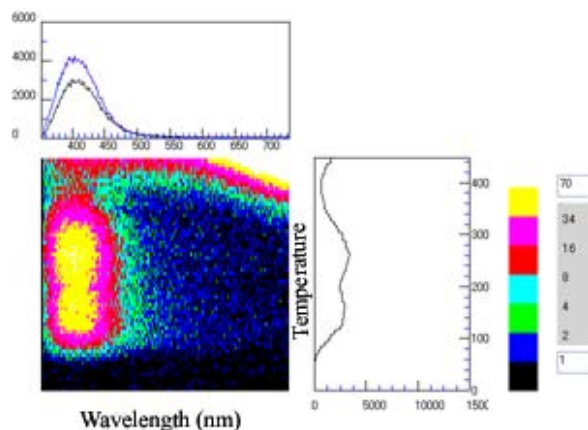


Fig.2. TL Spectra of a CR chondrite, Y981208 (CR2). TL intensity is displayed by pseudocolor.

REFERENCES:

- [1] D. W. G. Sears *et al.* Proceedings of Lunar and Planetary Science, **21**(1991) 493-512.
- [2] P. H. Benoit *et al.* Icarus **94**(1991) 311-325.
- [3] K. Ninagawa *et al.* Antarctic Meteorite Research, **11**(1998)1-17.
- [4] K. Ninagawa *et al.* Ant-arctic Meteorite Research, **15**(2002)114-121.
- [5] K. Ninagawa *et al.* Antarctic Meteorite Research, **18**(2005)1-16.

CO5-7 **Gamma-Irradiation Effect on Wasted Natural Agricultural Products (Coffee Beans, Indian Corns, and Rice Shells) toward the Re-Use Purpose**

M. Minagawa, M. Shimizu and N. Sato¹

Graduate School of Science and Engineering, Yamagata University

¹*Research Reactor Institute, Kyoto University*

INTRODUCTION: Previously we found that wasted coffee beans effectively absorb As from contaminated drinking water. Black-tea and green-tea showed no such results.¹⁾ Here we studied the mechanism by using WAXD, solid state NMR and ESR spectroscopies. In particular, ESR spectra showed the presence of many free radicals in coffee beans, which appear to be related to the absorption mechanism. The γ -ray irradiation effect on these 3 agricultural products was studied.

EXPERIMENTS: Only sample preparation procedure is described. The agricultural products were set in quartz tube (~100 ml) and heated under the following conditions: sample weight, 80 g; heating rate, about 10 °C/min; atmosphere, under imperfect oxidative conditions. The 3rd factor is very important to ensure good carbonized structure. The γ -irradiation experiments were carried out by using the γ -ray irradiation facility of Research Reactor Institute, Kyoto University.

RESULTS: It is possible to convert these 3 natural products to high-performance As absorber. The heating condition was quite important. The variations of sample weight and the absorbing property are clearly indicated (Fig. 1). Degradation took place in 2 steps, and beyond the latter temperature, the absorbing property suddenly appeared. This degradation-absorption relationship was observed commonly in the above 3 natural products.

Fig. 2 shows WAXD pattern, which indicates the destruction of core texture (cellulose main chain). The structural regularity notified by averaged intermolecular distance (4.2Å) disappeared completely. Solid state NMR results support this conclusion, although it is not presented here.

ESR spectra showed the existence of a lot of free radicals in the bulk sample (Fig. 3). The significant difference between middle and bottom curves should be noted. The latter sample showed extremely strong ESR signals, which appear to be related to the specific As absorption property. From a simple calibration curve using DPPH (diphenyl picryl hydrazil), we can estimate the radical concentration in the bulk sample. This step is now under investigation.

REFERENCES:

1)M. Minagawa, S. Ota, T. Ishikawa, J. Yatabe, H. Akashi; Preprints. of 9 Chem. and Related Societies of Tohoku Area of Japan, Koriyama, Sept. 21, 2009, p111.

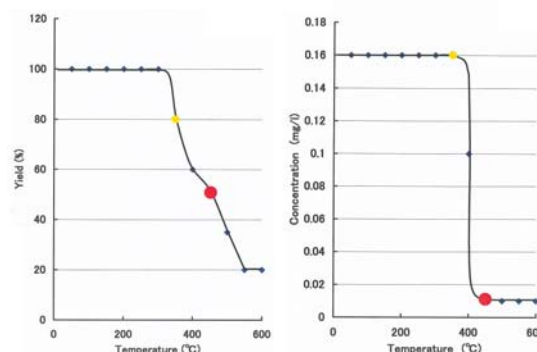


Fig.1. Wt. loss curve (left) and As absorption results(right) for Indian corns during heating process.

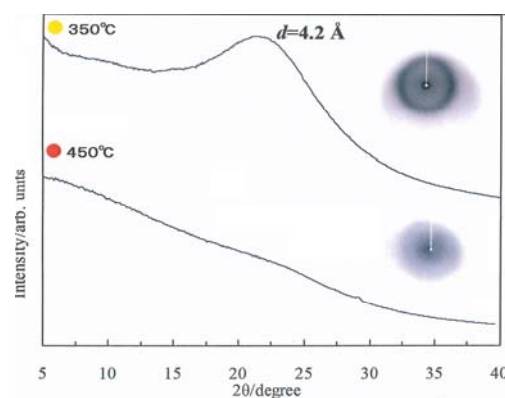


Fig.2. Comparison of WAXD pattern for heat-treated Indian corns up to different high temperatures.

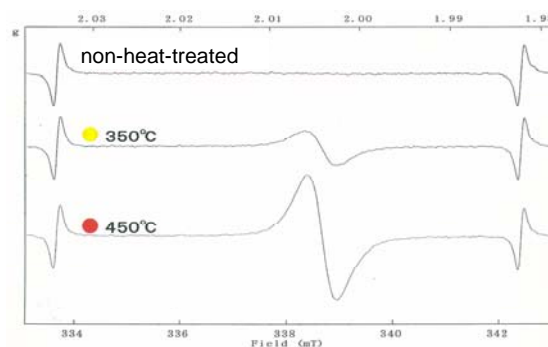


Fig.3. Comparison of ESR spectra for heat-treated Indian corns. Spectrum of non-heat-treated sample is also given.

CO5-8 Cathodoluminescence Study of Nanodiamond Formation in Meteorites

H. Nishido

Research Institute of Natural Sciences,
Okayama University of Science,

INTRODUCTION: The origin of the diamond particles in a planetary nebula has been debated for many years. Primitive chondritic meteorites contain up to ~1500 ppm of nanometer-sized diamonds. These nanodiamonds were recognized as presolar because of the isotopically anomalous noble gases that they involve. However, the origin of meteoric nanodiamonds is still very much an open issue. One early idea was that nanodiamonds were produced by high-pressure shock metamorphism of graphite through grain-grain collisions during the passage of interstellar shocks, whereas this process is not expected to be efficient because of not accompany of a large amount graphite. In recent years, other ideas have suggested that graphite grains might be induced to transform to diamond by intense particle irradiation, of which neutrons could be released from deep in the exploding star.

We conduct neutron implication experiments on graphite to clarify the formation mechanism of nanodiamonds by assuming neutron irradiation process at the KURRI. Cathodoluminescence (CL) could detect characteristic emissions from nanodiamonds if they would aggregate up to several hundreds nanometers. The main purpose of this study is to establish a CL experimental data on the synthetic nanodiamond particles that could be used for the astrophysical interpretation of the planetary nebulae. For comparison of natural diamond CL to synthetic one, luminescent characterization combined with micro-Raman spectroscopy were carried out for various diamond occurred in meteorites.

SAMPLES AND METHODS: Ureilite (Sahara 6235) newly found from Fezzou, Morocco were selected for CL and Raman measurements. Their polished thin sections with 20 μm thickness were preliminary examined under a polarized microscope to clarify the petrologic textures indicating carbon materials. Their surfaces were finished using silicon colloidal with a grain size of 100 nm, and coated with amorphous carbon.

CL spectra were obtained using a scanning electron microscope-cathodoluminescence (SEM-CL), which comprises the SEM (JEOL: JSM-5410) combined with a grating monochromator (Oxford: Mono CL2). The SEM-CL system was operated at 15 kV accelerating voltage and a probe current of 1.5 nA. CL spectra were recorded in the wavelength range of 350-800 nm with 1 nm spectral resolution and a dwell time of 1 second per step by photon counting. All CL spectra were corrected for total instrumental response. Raman spectra were obtained from the polished samples using a laser Raman microscope (JASCO: NRS-2100) located at the KURRI.

RESULTS & DISCUSSION: We could successfully detect sub-micron size grain of diamond in carbon materials in ureilite meteorite as CL emission image (Fig. 1), whereas Raman analytical method has been almost impossible to find such minute size diamond embedded in bulk carbonaceous materials. Bulk composition of carbon, hydrogen and sulfur are 3.34wt%, 0.12wt% and 0.17wt%, respectively. Nitrogen and carbonate carbon contents were under detection limit (<0.01wt%). Organic matter was not detected by py-GC and py-GC/MS. Carbon and oxygen stable isotope ratios are as follows; $\Delta^{13}\text{C} = -2.35 \pm 0.07 \text{‰}$. (vs. PDB), $\Delta^{17}\text{O} = 3.98 \pm 0.57 \text{‰}$ and $\Delta^{18}\text{O} = 8.08 \pm 0.47 \text{‰}$ (vs. SMOW). Oxygen isotope values are similar to those of ureilites previously reported and plot close to the CCAM line (carbonaceous chondrite anhydrous minerals).

The Raman peaks for diamond in the ureilite (a) range from 1334cm^{-1} to 1336cm^{-1} . Fine-grained olivine grains in the mesostasis show broad CL spectra around 640nm, 720nm and 800nm, probably due to Mn^{2+} , Cr^{3+} and lattice defects from Cr, respectively. Diamond grains have CL spectral peaks at 420nm, 520nm and 620nm (Fig. 2), which are similar to those of ureilite previously reported. The CL peaks of these diamonds are completely different from those of terrestrial ones, and consistent with those of diamonds from impact craters. A diamond-related 520 nm broad peak was also observed at NGC 7026 and NGC 7027 planetary nebulae, which are C-rich objects. It suggests that the diamonds in the ureilite were generated from graphite precursors by the impact of celestial bodies in the solar system. This indicates the presence of nanodiamond dust particles in the dust matter of these nebulae, which may be originated due to ejection of the outer parts of the Red Giants during planetary nebula formation.

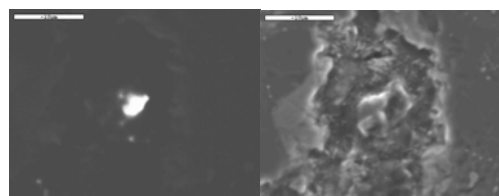


Fig. 1. CL image of micro diamond in ureilite (left), SEM image of cluster carbon materials (right). Scale: 10 μm .

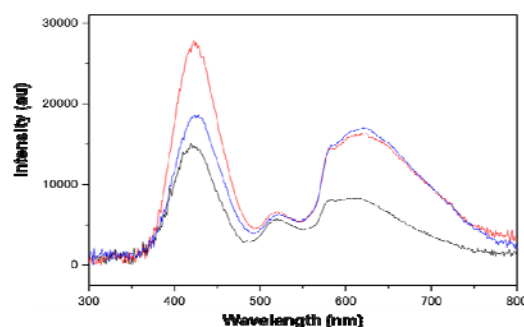


Fig. 2. CL spectra of micro diamond in ureilite.

M. Ebihara and S. Sekimoto¹

Graduate School of Science, Tokyo Metropolitan University

¹*Research Reactor Institute, Kyoto University*

INTRODUCTION:

It is important to know the elemental composition in meteorite samples for discussing the classification, formation mechanism and metamorphism of those samples. However, the behavior of the halogen elements in formation and metamorphism of meteorites have rarely been studied in detail because accurate and reliable data about the abundances of halogens in meteorites have scarcely been obtained.

Radiochemical neutron activation analysis (RNAA) has been used for determination of trace amount of chlorine, bromine and iodine in meteorite and geological standard rock samples [1-7]. In terms of accuracy and sensitivity in analysis of those three halogens, RNAA is the best method among various analytical methods.

In this work, we tried by RNAA using Kyoto University Reactor (KUR) to determine the trace amount of chlorine, bromine and iodine in sedimentary rock samples whose Cl, Br and I contents was reported as only preferable values or have never been reported, to confirm that RNAA using KUR is applicable for analysis of those halogens in meteorite samples.

EXPERIMENTS:

The sedimentary rock samples analyzed in this work are JLk-1, JLs-1, JDo-1, JSI-1, JSI-2, JSd-1, JSd-2, JSd-3 and JCh-1, which are commercially available in National Institute of Advanced Industrial Science and Technology. About 100 mg of each sample was weighed out in a small plastic vial, which had been washed with ethanol, and then the vial was sealed in a clean polyethylene bag. As the reference standard, chemical standards were prepared for such elements as chlorine, bromine and iodine. Appropriate amounts of standard solution of these elements were dropped onto filter papers, which were then dried under an infrared lamp.

Generally, two rock samples were irradiated with a set of reference standards of Cl, Br and I at each run. The neutron irradiation was carried out for 10 min using the pneumatic transport system (Pn-1) of KUR. After the irradiation, the samples were cooled for a few minutes and subjected to radiochemical treatment for the separation of I-fraction and Cl- and Br-fractions.

A known amount of each halogen carrier solution (10 mg for Cl, 20 mg for Br or 30 mg for I) and saturated NaOH solution were placed with carrier solution of manganese in a nickel crucible, and heated to dryness. The irradiated rock sample was immediately transferred into the crucible including the above carriers and fused

with about 1 g of NaOH. The crucible was heated mildly for the first few minutes and strongly for 5 min after melting of the flux. After the heating for fusion, the fused cake was dissolved in water. The hydroxide precipitation was separated from the supernatant solution including chloride, bromide and iodide ions by centrifugation. A few mg of sodium sulfite was added to the solution to reduce iodate ions to iodide ones. The solution was made slightly acidic with 6M HNO₃. The black solid of PdI₂ was precipitated by adding a solution of Pd(NO₃)₂. The precipitate was separated from the solution including chloride and bromide ions by filtration and washed with 0.2M HNO₃ to remove sodium and manganese containing ²⁴Na and ⁵⁶Mn, respectively which raised the background in the γ -ray counting. The precipitate as PdI₂ was collected on a filter paper and dried under a lamp. To the solution including chloride and bromide ions, a solution of AgNO₃ was added to obtain the precipitates of AgCl and AgBr. Those precipitates were also washed with HNO₃, collected on a filter paper, and then dried under a lamp. Finally, both precipitates of PdI₂ and AgCl or AgBr were fixed with a cellophane tape and subjected to γ -ray measurements of ¹²⁸I and ³⁸Cl or ⁸²Br.

Chemical yields of the above procedure were determined by neutron activation method. After the γ -ray measurements were completed, the precipitates of PdI₂ and AgCl or AgBr were irradiated for ten seconds using Pn-1 of KUR with the reference standards which were prepared from the standard solution. The same nuclides and γ rays in the measurements were used to determine the chemical yields, which were estimated to be approximately 90%, 80% and 60% in average for Cl, Br and I, respectively. Those yields obtained in this work were similar to those in the previous experiments[4, 5].

RESULTS:

The contents of Cl, Br, and I in the nine sedimentary rock samples have been determined more than twice. Evaluation of those data is in progress. The final data obtained in this work will be published to the scientific journal in the field of geochemistry

- [1]T. Nakamoto *et al.*, *Anal. Sc.* 23 (2007) 1113-1119.
- [2]H. Ozaki and M. Ebihara., *Anal. Chim. Acta.*, **583** (2007)384-391.
- [3]F. Kato *et al.*, *Antarctic Meteorite Res.*, **13**(2000)121-134.
- [4]M. Ebihara *et al.*, *J. Radioanal. Nucl. Chem.*, **216** (1997) 107-112.
- [5]T. Shinonaga *et al.*, *Chem. Geol.* **115** (1994) 213-225.
- [6]T. Shinonaga *et al.*, *Geochim. Cosmochim. Acta* **58** (1994) 3735-3740.
- [7]M. Ebihara *et al.*, *Anal. Sci.* **8** (1992) 183-187.

H. Tsukada, A. Takeda, N. Akata, H. Kakiuchi, S. Fukutani¹ and T. Takahashi¹

Department of Radioecology, Institute for Environmental Sciences

¹Research Reactor Institute, Kyoto University

INTRODUCTION: Radionuclides in soils after deposition can play an important role in the change of the physicochemical form, which is an important factor in determining the fate of radionuclides in the environment. Iodine is an essential element for animals and humans. It is well known that iodine is needed for the synthesis of thyroid hormones and that iodine deficiency induces thyroid diseases. Radioiodine (including ¹²⁹I and ¹³¹I) released from nuclear facilities is of special concern because of its high fission yield, volatility, transferability, and its ability to accumulate in the human thyroid. The pathway of radioiodine from soil to the human bodies via soil plant (agricultural products) is one of the important processes [1].

The chemical states of iodine in environment are iodide (I⁻) and iodate (IO₃⁻). The solution-to-spinach leaf transfer factor of iodate is higher than that of iodine [2]. On the contrary, the solution-to-water spinach transfer factor increased in the order of CH₂ICOO⁻ > I⁻ >> IO₃⁻ solutions when the concentration of iodine in the solutions was over 0.1 mg I/l [3]. These results suggest that transfer of iodine from soil to plant is different among iodide, iodate and other forms. However, only a little is known about the transport mechanism of iodine by plant from soil.

The present study investigates root uptake of iodine depending upon the concentration of iodine (iodide and iodate) in the water culture, and the distribution of iodine in shoot and root part.

EXPERIMENTS: Orchardgrass (*Dactylis glomerata*) was used as a model plant. A hydroponic experiment was carried out to investigate the transport of iodine from water to plant. The orchardgrass was grown in solution containing 2 mM KNO₃, 2 mM NH₄NO₃, 2 mM MgSO₄, 0.6 mM CaCl₂, 0.5 mM KH₂PO₄, 25 μM FeNaEDTA, 10 μM H₃BO₃, 2 μM MnSO₄, 1 μM ZnSO₄, 0.2 μM CuCl₂, 0.05 μM Na₂MoO₄. After the orchard grass was grown for 7 days, iodine (I⁻ or IO₃⁻) was added in the solution as 2, 20 200, and 2000 mg L⁻¹. The leaves were harvested after more 2 days, and they were freeze-dried. The dried samples were pulverized with an agate ball mill.

Concentration of iodine in the samples was determined by instrumental neutron activation analysis (INAA). The samples were sealed in polyethylene bags, and a numbers of bags were put into a polyethylene capsule. The capsules were irradiated in the Kyoto University Research Reactor (Pn-3) at a thermal neutron flux rate of 4.9×10^{16}

n m⁻² s⁻¹ for 150 seconds. The samples were cooled for a couple of minutes after irradiation and then counted by means of Ge detectors for 100-500 seconds.

RESULTS: Inhibition of plant growth was not observed by root uptake of iodine during 2 days. Relationship between concentration of iodine in the plant determined by INAA and iodine concentration in culture solution is shown in Fig. 1. The concentration of iodine in the samples increased with increasing iodine concentration in culture solution. The concentration of iodine in plant samples varied about two orders of magnitude when the iodine concentration in the water culture varied three orders of magnitude. The concentration of iodine in the plant added as I⁻ in the solution was higher than that added as IO₃⁻. The iodine concentration in the root was higher than that in the shoot when iodine was added as IO₃⁻. However the concentration of iodine in the both parts was relatively similar value in the addition as I⁻. The results indicate that the root uptake of I⁻ can be easier than that of IO₃⁻.

The plants were cultivated in the water culture added as I⁻ or IO₃⁻, and the chemical form of iodine in the samples was determined by L_{III}-edge X-ray absorption near-edge structure fingerprinting method. Dominant chemical form of iodine was I⁻ in the orchardgrass (both in shoot and root) even if the iodine chemical forms in the nutrient solution was different. It is attribute that iodate would be transferred into plant root after reduction to I⁻.

REFERENCES:

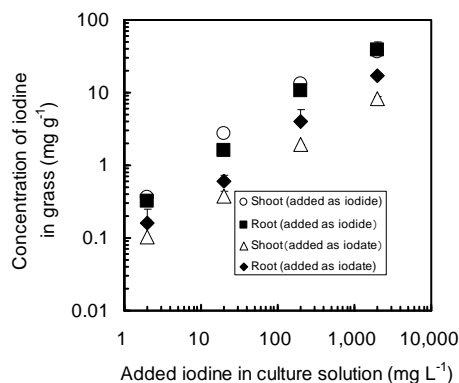


Fig. 1. Relationship between concentrations of iodine in orchardgrass and culture solution.

- [1] Y. Muramatsu *et al.*, J. Radiat. Res., **24** (1983) 326-338.
 [2] Y.-G. Zhu *et al.*, Environ. Int., **29** (2003) 33-37.
 [3] H.-X. Weng *et al.*, Bio. Trace Elem. Res., **124** (2008) 184-194.